SOVIET PHYSICS USPEKHI VOLUME 15, NUMBER 4 JANUARY-FEBRUARY, 1973

537.58

MASS ANALYSIS AND FIELD-ION MICROSCOPY

A. L. SUVOROV and V. V. TREBUKHOVSKIĬ

Institute of Theoretical and Experimental Physics

Usp. Fiz. Nauk 107, 657—683 (August, 1972)

The review discusses methods of mass-spectrometric analysis of particles extracted from a field-ion microscope, for the purpose of developing the theory and practice of field-ion microscopy research. The theoretical and experimental aspects of the probe-analysis procedure are discussed. The results of the principal work done in this field are used for the purpose of extending the existing ideas concerning the autoionization, field-evaporation, and formation of field-ion images.

CONTENTS

1. INTRODUCTION

A reasonable unification of several procedures of physical (or other) research, or a partial transfer of some fundamental features of one procedure to another, can greatly extend the capabilities of any particular method and make it applicable to new prospective research fields. This fact is obvious and can be confirmed by many examples. One of the examples of such a fruitful cooperation, the combination of mass spectrometry[1] and field-ion microscopy[2,3a] is the subject of the present review. Whereas the use of autoionization, on which the operation of the field-ion microscope is based, for purposes of ion production in mass spectrometry has greatly extended the capabilities of the mass-spectrometric analysis of particles artificially extracted from the field-ion microscope gives an inestimable contribution both to the development of field-ion microscopy procedures and to the understanding of the processes that take place in strong electric fields. Both approaches are presently undergoing vigorous development. The first is the subject of the basic research of Beckey[4], Robertson[5], and Gol'denfel'd and coworkers[6]; the second has been most successfully developed in the laboratory of Müller[3c,d,7], the inventor of field-ion microscopy, and also by Brenner and McKinney[8a]. It should also be noted that it is very difficult and not always possible to draw a distinct boundary between them, i.e., to say definitely which work in this field is more useful for the development of field-ion microscopic or mass-spectrometric procedures. Nonetheless, since field-ionization mass spectrometry is a rather extensively and sufficiently independent branch of physico-chemical research, its consideration together with problems of field-ion microscopy is apparently desirable. This problem loses its significance also in connection with the recently published monograph by Beckey[4b], devoted entirely to numerous aspects of field-ionization mass spectrometry. The authors therefore wish to stipulate immediately that the present review, written from the point of view of the field-ion microscopy expert, intends primarily to describe the progress made in field-ion microscopy through the use of mass-spectrometry techniques. Certain theoretical problems are also considered from similar points of view.

2. AUTOIONIZATION

At the present time autoionization, or ionization of an atom in a strong electric field by the tunnel effect, is recognized to be the basis of the mechanism of image production in the field-ion microscope[2,3a,b,8a]. The tunnel mechanism of passage of an electron through a potential barrier was first proposed by Gamow to explain radioactive alpha decay in his work on the quantum theory of atomic nuclei[10]. At the same time, Oppenheimer[11] has drawn the conclusion that a valence electron of an atom in an electric field has a probability of tunnelling through a potential barrier that is lowered by the field. The electric field intensities necessary to attain a realistic autoionization probability, calculated by Oppenheimer, turned out to be in good agreement with the experimental value corresponding to the start of ion production in the ion field microscope. The first rigorous analysis of autoionization from the point of view of quantum mechanics was made by Lanczos[12], who obtained for the case of hydrogen data that are in good agreement with experiments on the study of the decrease of the intensity of spectral lines in strong electric fields (the Stark effect). This question is discussed in detail in a review by Bethe and Salpeter[13], devoted to the quantum-mechanical analysis of single- and two-electron systems. The first to examine the autoionization process as applied to the field-ion microscope, within the framework of a one-dimensional model of the potential barrier, were Good and Müller[14], who used the WKB expression for the

transparency of the barrier[15]. The probability B of tunneling of an electron from an atom located at a metallic surface into a field of intensity F is given in this case by

$$D = \exp\left[-(8m_e/\hbar^2)^{1/2}\int_{x_2}^{x_1}(V_e - E_e)^{1/2}\,dx\right], \qquad (1)$$

where E_e is the total electron energy, m_e is the electron mass, $\hbar$ is Planck's constant divided by 2π, and the electron's potential P_e at a distance x from the metallic surface can be approximately written in the form

$$V_e(x) = -e^2 \mid x_i - x \mid^{-1} + Fex - (e^2/4x) + e^2(x_i + x)^{-1};$$

where e is the electron charge. The first term in this expression corresponds to the Coulomb attraction of an ion at a distance x_i from the surface of a metal, and the last two terms are the potentials corresponding to the images of the electron and ion in the metal. The probability dP_i for an ion to be ionized in a layer dx is

$$dP_i = (dx/v_r)\tau_i(x),$$

where v_r is the atom velocity in a direction perpendicular to the surface of the tip, and τ_i is the ionization time of the atom at a distance x from the surface:

$$\tau_i = 1/\nu D.$$

In the last expression, ν is the frequency with which the electron of the atom collides with the potential barrier. The autoionization probability increases when the atom approaches the metallic surface, reaching a maximum at a critical distance x_c determined by the Pauli principle and corresponding to equality of the energy level of the valence electron of the atom to the Fermi level of the metal. This case is illustrated in Fig. 1b. If we consider the atom in free space (Fig. 1a) in the form of a potential well of depth equal to the ionization potential, on the bottom of which there is located a valence electron, then Fig. 1b represents its distortion in a strong electric field in free space, and Figs. 1c and 1d show the distortion at the surface of the metal. The increase of the transparency of the barrier near the metallic surface, due to the action of the image forces, makes the probability of autoionization near the metallic surface appreciable, whereas in free space, at the same field-intensity value F, the probability is negligible.

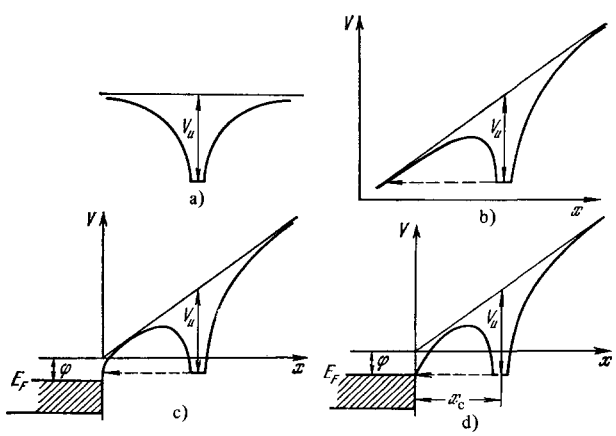

FIG. 1. Potential curves of electron in free space without a field (a), in the presence of a field (b), and in a strong electric field at the surface of a metal (c, d).

Quantum mechanical theories of autoionization of an atom (hydrogen) near a metallic surface, within the framework of the three-dimensional model of the potential barrier, were proposed by Boudreaux and Cutler[16] (they are also given in the paper of Sharma et al.[17], who consider the probability of electron tunneling as a function of the structure of the Fermi surface for different crystallographic planes). To this end, they investigated in succession a variational method[16a], time-dependent perturbation theory[16b], and a particular case of the theory of atomic collisions[16c]. In the second case, the probability P_i of tunneling of an electron through a potential barrier (ionization) is proportional to the square of the M* matrix element of the perturbation:

$$\mid M^* \mid^2 = \mid \langle \Phi_\alpha \mid V' \mid U_0 \rangle \mid^2,$$

where Φ_α and U_0 are the wave functions of the electron in the metal and in the atom (at large distances from the metallic surface), respectively, and V′ is a perturbing potential that can be represented approximately in the form of a sum

$$V' \approx V_e + V_{II} + V_p;$$

here V_e is the potential energy of the interaction of the electron with the metal, without account of the effects due to the presence of the ion core, but including quantum mechanical forces, V_{II} is the potential energy of the interaction of electron with the image of the ion in the metal, while V_p is the potential energy of the electron in the field F and is equal to F at $x \geq 0$ and to zero at $x < 0$.

Another theoretical analysis was carried out by Boudreaux and Culter under the assumption that in autoionization the atom collides with an infinitely heavy metallic tip (having a perfectly smooth surface), in which the particle redistribution causes the electron of the atom to remain in the metal. The autoionization process was expressed briefly in the form

$$A + B \rightarrow C + D,$$

where A is the atom, B the metal, C the metal receiving the electron, and D the ion. In the cited paper[16c], using the case of general collision theory with redistribution of the particles[18], they employed the first Born approximation. All these theories confirm qualitatively the presently assumed picture of formation of ion images[2]. In addition, numerical calculations carried out in accordance with these theories are in satisfactory agreement with the fundamental experiment of Tsong and Müller[19a], who revealed the existence of so-called ionization bands, located at a critical distance x_c from the surface of the tip over the most strongly projecting surface atoms. According to[19a], these bands are disk-shaped regions with diameters of several tenths of an angstrom. Their half-width calculated from experiment was 0.2 Å. In addition, it turned out that it is not constant, but increases with increasing field intensity (see Fig. 2, where the arrow indicates the voltage corresponding to the best-image conditions). The one-dimensional model of Good and Müller yields for the ionization-band half-width a value 0.4 Å, whereas the values given by the three-dimensional theories of Boudreaux and Cutler lie in the range 0.11—0.12 Å. Figure 3 shows by way of example the peak of the field-ion distribution,

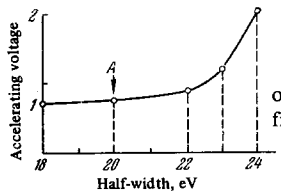

FIG. 2. Dependence of the half-width of the ionization band on the electric field intensity (voltage at the tip) [3a].

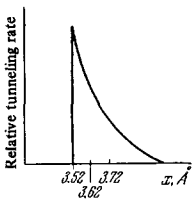

FIG. 3. Theoretical distribution of field ions [19b].

corresponding to the aforementioned theories and to the experimental data obtained in[19a]. The critical distance corresponding to this case is $x_c = 3.52$ Å (the probability of autoionization becomes equal to zero for distances shorter than x_c).

The following, however, must be noted concerning these investigations. As is well known, neither the variation method nor perturbation theory is sensitive to the asymptotic behavior, i.e., while adequate for the determination of the energies, they can result in an appreciable error when it comes to determining the electron tunneling probability. Therefore even an increase in the parameters, which undoubtedly is useful, will not make it possible to estimate the possible errors, which may turn out to be quite high. In addition, the realization of the results of three-dimensional quantum-mechanical autoionization theories[16] encounters great computational difficulties. On the other hand, the analytic expression presented here (see Eq. (1)) is based on a one-dimensional model that does not take into account the spherical symmetry of the particle and the planar symmetry of the metal. Nor does the one-dimensional approach make it possible to estimate correctly the absolute value of the amplitude of the tunneling probability distribution peak. It is therefore necessary to stop and discuss in greater detail the three-dimensional autoionization theory proposed (for the hydrogen atom) by Gol'denfel'd et al.[20] Unlike Boudreaux and Cutler, Gol'denfel'd et al.[20] succeeded in obtaining an analytic expression for the autoionization probability.

The employed differential equation for the ionization probability was an expression for the difference between the electron fluxes into and from the metal. If β is the probability of filling the electron vacancies in the atom and $1-\beta$ is the probability of the ionic state, while γ is the analogous quantity for the metal, then the indicated difference is equal to the increment $-d\beta$ of the ionic state, i.e.,

$$-d\beta = (\beta - \gamma)\,\Xi\,dt\ ^{*}). \qquad (2)$$

The quantity Ξ, which the authors of[20] called the ionization rate constant (IRC), is equal to the total probability flux of the passage of the electron through the potential barrier. In its sense, it is equal to the reciprocal mean lifetime of the particle arriving at the metallic surface in the neutral state. It should depend only on the field intensity F and on the distance x to the surface of the metal.

The energy distribution of the ions (the ion current produced at a distance x from the surface of the metal) is written in the form

$$j(x) = d\beta/dx = (\gamma - \beta)\,n(x)\,\Xi/v(x), \qquad (3)$$

where v(x) is the particle velocity and n(x) is the particle flux, equal to

$$n(x) = 2r_0^2 n_0 (2\pi kT/m)^{1/2}\{1 + [\mu F(x) + 0.5\alpha_{par} F^2(x)]\,(kT)^{-1}\}.$$

in this expression, n_0 is the concentration of the neutral particles in the absence of the field, r_0 is the radius of the needle, m, μ, and α_{par} is the mass, dipole moment, and polarizability of the particle, respectively, k is Boltzmann's constant, and T is the absolute temperature of the tip.

Since Eqs. (2) and (3) can be regarded as equations for one variable x, we have

$$\beta = \beta_0 \exp\left(\int_{x_0}^{x} \Xi v^{-1}\,dx'\right) + \left[\exp\left(-\int_{\infty}^{x} \Xi v^{-1}\,dx'\right)\right] \times \int_{x_0}^{x} \left[\Xi v^{-1}\gamma \exp\int_{\infty}^{x_1} \Xi v^{-1}\,dx''\right]\right] dx'.$$

As a result, the entire problem reduces to the determination of the explicit form of the IRC.

If the ψ-function of the electron in the system is known, then the IRC can be obtained by integrating the probability flux density $(0.5[\psi\nabla\psi^{*} - \psi^{*}\nabla\psi])$ over a suitably chosen surface. The main difficulty lies here in the fact that it is impossible to obtain an exact expression even for the simplest case of the hydrogen atom in a homogeneous electric field. Approximate analytic solutions for such a case were obtained by a number of workers. Rice and Good[21] have shown that the best solutions are those of Lanczos[12a] and of Landau and Lifshitz[22]:

$$\Xi = (4/Fn^3)\exp(-2/3Fn^3), \qquad (4)$$

where n is the principal quantum number. Since it turned out that the solution of the problem in question is determined mainly by the behavior of the ψ-functions of electrons far from the nucleus, and the asymptotic approximations of the ψ-functions in complex particles are hydrogen-like, the authors of[20] used for them an expression similar to (4):

$$\Xi = 4F^{-1}(2V_i)^{3/2}\exp[-2(2V_i)^{3/2}/3F],$$

where V_i is the ionization potential of the particle.

The influence of the metallic boundary on the ionization probability was taken into account by the authors of[20] by introducing image forces in the Schrödinger equation for the system "hydrogen atom + field + metal." This equation was solved in[21] by a method described by Landau and Lifshitz[22]:

$$\Xi = (4/F)(2V_i)^{3/2}(1-a)(1+a)^{-1}\exp[b\{\operatorname{arctg}[(1-a)(1+a)^{-1}] - \operatorname{arctg} b^{-1}\}] \times \Phi(F', x_0)\exp\{-[2(2V_i)^{3/2}/3F](1-a^3)\},$$

where

$$\Phi(F', x_0) = [(a+c_1)(1-c_1)/(a-c_1)(1+c_1)]^{1/2c_1} \text{ for } x_0 < 1/2F',$$
$$\Phi(F', x_0) = \exp[c_2 \operatorname{arctg} c_2 - c_2 \operatorname{arctg} c_2 \cdot a)] \text{ for } x_0 > 1/2F',$$
$$\Phi(F', x_0) = \exp(F^{-1/4} - 1) \text{ for } x_0 = 1/2F',$$

[1)] Equation (2) and all the following expressions in this section are given in atomic units.

$a = (1 - F'\eta_1)^{1/2}$, $b = (4F'x_0 - 1)^{1/2}$, $c_1 = (1 - 2F'x_0)^{1/2}$, $c_2 = (2F'x_0 - 1)^{-1/2}$, $\eta_1 = \eta_1^0 + 2(2r_0 - \eta_1^0)(2V_i)^{-1/2}[2F'\eta_1^0 + (c_2+2)^{-2}]^{-1}[(\eta_1^0)^{-1} - 2\cdot(4x_0 - \eta_1^0)^{-1}]$, $\eta_1^0 = (1/2F')[(2+c_2)^{-2} - (c_1^4 + 2F'V_i^{-1})^{1/2}]$,

$$F' = F/2V_i.$$

The obtained expressions show that the average lifetime of the particle in the neutral state depends very strongly on the field intensity F. In fields corresponding to the conditions where the best image in the field-ion microscope is produced, the ionization, as already mentioned, occurs near the surface of the metal (at a distance x_c) in a very narrow band. For such fields, the half-width of the ionization band coincides with the half-width of the IRC, that is, $\Xi(x_c) = 2\Xi(x_c + \Delta x)$. Then, according to[23],

$$\Delta x = 0.693\,[(\varkappa^2 + F_0)/2V_i]^{1/2}\,[\varkappa + (\varkappa^2 + F_0)^{-3/2}], \qquad (5)$$

where

$$\varkappa = 0.5\{1 + \varphi V_i^{-1} - [(1 - \varphi V_i^{-1})^2 + F_0 V_i^{-2}]^{1/2}\},$$

F_0 is the field at the top of the tip and φ is the work function. The value of Δx calculated from (5) is ~ 0.3 Å.

In higher-intensity fields the influence of the metallic surface becomes smaller, and, as shown by experiment, a new effect comes into play (we have in mind the appearance of the autoionization structure, observed by Jason et al.[23,24] and explained by Jason[25]; it will be considered in Sec. 4).

A further increase of the field intensity causes the ionization to begin to take place entirely—at a considerable distance from the surface of the tip, i.e., on the direct path of the neutral particles towards the tip (ionization in the "volume").

3. FIELD EVAPORATION

The great possibilities of the field-ion microscope were discovered after Müller[3e] observed the phenomenon of evaporation of atoms and molecules adsorbed on the surface of the tip (desorption by the field; see, for example,[26]), and also evaporation of the matrix atoms under the influence of strong electric fields (evaporation by the field). The discovery and study of this phenomenon has made it possible to remove in controlled fashion in the field-ion microscope layer after layer of specimen surface atoms, and investigate the specimen structure throughout its volume. Field evaporation was considered in detail in a number of papers (for example,[27-30]), in which various models of this process are described. The activation energy Q_n for evaporation in the presence of an electric field of intensity F is given by[3a]

$$Q_n = \Lambda + \sum_n V_i^{(n)} - n\varphi - (n^3e^3F)^{1/2}, \qquad (6)$$

where n is the charge of the evaporated ion, Λ is the heat of sublimation of the metal atom (for the case of evaporation of the specimen itself), and $V_i^{(n)}$ is the n-th ionization potential of the metal atom. Expression (6) corresponds to the so-called image potential model, which is illustrated by the potential curves on Fig. 4 (the atomic curve is shown solid and the ionic one dashed). In this case, the atomic state is stable and the atomic and ionic curves intersect on the left of the barrier of the image potential. Without a field we have

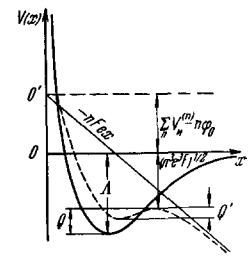

FIG. 4. Schematic representation of the potential energy curves, corresponding to the transition of an atom to the ionic state followed by evaporation through the barrier of the image potential [27b].

$$Q_0 = \Lambda + \sum_n V_i^{(n)} - n\varphi_0. \qquad (7)$$

The evaporating field is defined in accordance with[3a]

$$F_{ev} = n^{-3}e^{-3}[\Lambda + \sum_n V_i^{(n)} - n\varphi + 0{,}5\,(\alpha_{par} - \alpha_i)F_{ev}^2 - kT\ln(\tau/\tau_0)], \qquad (8)$$

where τ is the time required for evaporation, τ_0 is the period of the oscillation of the free surface atom, α_{par} and α_i are the polarizabilities of the atom and ion, respectively. Consequently, if we start from (7), the condition of field evaporation can be written in the form

$$Q_0 \leqslant (n^3e^3F)^{1/2}.$$

The rate k_{ev} of field evaporation is determined by the Arrhenius equation[27b]. At high temperatures, when the tunnel effect can be neglected, k_{ev} is given by

$$k_{ev} = \nu \exp(-Q_n/kT);$$

here ν is the oscillation frequency of the surface atoms. When the temperature is lowered, an increasing role is assumed by electron tunneling. For the case of low temperatures, Tsong[28], using the WKB approximation and replacing the potential barrier at the surface of the metal by a triangle with height Q_n and with lateral sides s and s', obtained

$$k_{ev} = \nu \exp[-4/3\,(2M/\hbar^2)^{1/2}(S^{-1} - |S'|^{-1})Q_n^{3/2}]\,\text{sec}^{-1} = \nu \exp(-aQ_n^{3/2});$$

here $a = (4/3)(2M/\hbar^2)(S^{-1} - |S'|^{-1})$ determines the tunneling probability, and M is the mass of the evaporated atom or complex. According to[2], with certain assumptions, the most acceptable for k_{ev} is the expression

$$k_{ev} = \nu p \exp\{Q_n/kT + [4/27a^2(kT)^3]\},$$

where p is a function that depends little on T and F. For practical purposes, p can be regarded as constant.

As a result, the field dependence of the rate of evaporation at constant temperature takes the form

$$\left(\frac{\partial \ln k_{ev}}{\partial \ln F}\right)_T \approx \frac{bQ_0}{2kT} + \frac{4}{3}\left(\frac{2M}{\hbar^2}\right)^{1/2}\frac{\Delta_0^{3/2}}{neF}.$$

In this expression $b \equiv [1 - 2(\alpha_{par} - \alpha_i)F^2]/Q_0$, $\Delta_0 = 4/9a^2(kT)^2$.

When speaking of evaporation by the field, mention should be made of another approach, proposed by Dobretsov and Ionov[30], to the solution of the problem, namely to an analysis of the evaporation and desorption of the ions in the electric field within the framework of the surface-ionization theory. According to[38], the evaporating fields can be obtained in this case from the equations

$$e(eF)^{1/2} \approx I_{+0}^0[(1 - (T/T_i)] \text{ for } F < F_c$$

and

$$eFx_c \approx I_{+0}^0[1-(T/T_1)]-\lambda_{+0} \text{ for } F>F_c,$$

where I_{+0}^0 is the heat of desorption of the ions at F = 0, T_1 is the temperature at which an ion current $i_1 = i$ = const is emitted in the absence of a field, λ_{+0} is the work of the polarization forces on the path from $x = \infty$ to $x = x_c$, and F_c is the electric field intensity at which the force exerted on the ion by the field in the entire path from x_c to ∞ exceeds the forces directed towards the surface. We note that, unlike in the previously considered autoionization theories, x_c stands here for the critical charge-exchange distance[29].

In addition to the fact that the field evaporation makes it possible to investigate the structure of the sample inside its volume, it is an indispensible tool for final polishing of the tip and its purification to obtain atomic resolution of an atomically pure surface. However, the dependence of the rate of field evaporation on the electric field intensity (i.e., on the initial values of the local curvature of the sample) determines in part the fact that the final shape of the tip is far from a hemisphere and that the values of the local radii can differ by several times, being functions of the evaporation regime. In addition, as seen from[8a], the crystallographic faces of samples made from the same material at equal curvature radii have different evaporating fields, owing to the differences between their work functions. On the other hand, differences between the average evaporating field of different sample materials can determine the preferable field evaporation of atoms of one type in the case of field-ion microscopy of alloys.

4. MASS-SPECTROMETRIC INVESTIGATIONS OF THE AUTOIONIZATION PRODUCTS OF NOBLE GASES

Even the very first experiments by Inghram and Gomer[31], aimed at obtaining a mass-spectrometric analysis of ions produced in strong electric fields at metal surfaces, have shown that adsorption of the gas molecules by the metallic surface is not (as previously assumed) the essential condition for their ionization. It is precisely these results which have subsequently made the concept of autoionization mechanism of image production in a field-ion microscope the principal premise of the theory of this instrument. The indicated investigations were performed with an ordinary field-ion microscope having in its fluorescent screen an opening through which some of the produced ions entered the analyzer of an ordinary mass spectrometer. A more sophisticated variant of such an instrument was constructed by Müller and Bahadur[32], who introduced into the system electrostatic lenses to focus the ion beam. Subsequently, many variants of improved field-ion sources were developed, and commercial production of sources for mass spectrometers, in which the ions can be produced either by autoionization or by electron impact, became available in 1968.

Figure 5 illustrates the results of Inghram and Gomer[31a], which they obtained for the autoionization of hydrogen near a tungsten tip at a hydrogen pressure 3×10^{-4} mm Hg. The numbers next to the experimental points indicate the half-width of the peak in volts (the resolution of the instrument used in[31a] was ~ 20 V. The values of the field intensity F are decreased in the presented plot by one-half in comparison with the original, in accordance with Müller's correction[3a]. We see that formation of H_2^+ ions (curve 2 on Fig. 5) is favored in weaker fields and H^+ ions prevail in stronger fields. The latter corresponds precisely to the case of pure autoionization at short distances from the surface of the tip. The relative numbers of the different ions produced in autoionization of H_2 and D_2[31a] are listed in the table[31a]. The table gives also the values of F with allowance for Müller's corrections[3a] (see above). A very interesting experimental result was obtained by Jason et al.[23,24] in a mass-spectrometric investigation of the products of autoionization of molecular hydrogen on the surface of a tungsten tip. A definite structure was unexpectedly observed in the energy spectrum of the hydrogen ions produced in a strong electric field near a metallic surface (Fig. 6). In other words, it turned out that in autoionization of hydrogen the intensity of the ion current reaches a maximum value—it not only has a peak (see the large peak on Fig. 6b) for the H_2^+ ions produced in the ionization bands determined by Tsong and Müller[19], but in addition have peaks (the remaining peaks on Fig. 6b) corresponding to ionization at distances larger than x_c from the surface. It was earlier assumed, on the other hand, that most ions are produced in the ionization band (which in this case can be called the "first ionization band"), and

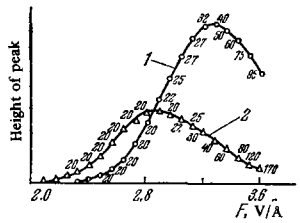

FIG. 5. Dependence of the height of the peaks of H^+ (1) and H_2^+ (2) on the applied voltage for autoinization of hydrogen [3a].

Analyzed gas	Component ions	Relative number of ions	Electric field intensity F, V/cm
H_2	H^+	0.5	2.8
	H_2^+	0.5	
D_2	D^+	0.5	2.8
	D_2^+	0.5	
	HD^+	0.025	

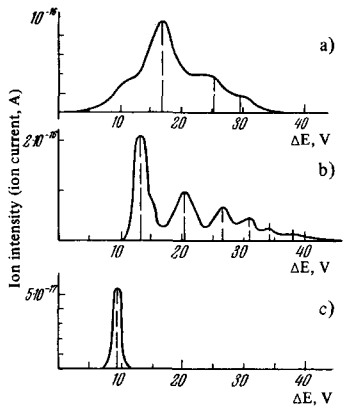

FIG. 6. Dependence of the total current of the field-emitted ions H^+ (a), H_2^+ (b), and H_3^+ (c) on the excess ΔE of the electron energy over the Fermi level [24].

then the number of produced ions decreases monotonically with increasing distance from the tip. The typical example of the energy distribution of the ions H^+, H_2^+ and H_3^+, obtained in[24] and shown in Fig. 6, corresponds to autoionization over the (110) planes. The first H_2^+ peak (Fig. 6b) is observed at an energy deficit (excess of electron energy over the energy corresponding to the Fermi level) $\Delta E = 11.7 \pm 0.3$ eV, and agrees with the peaks obtained by Tsong and Müller[19a]. As proof that the observed structure really exists and is not the product of the experimental procedure, the authors of[24] cite the following arguments: such a structure was clearly observed only for H_2^+, less clearly for H^+, and is completely absent for H_3^+; the structure depends on the field and not on the focusing, the finish of the tip, and the residual-gas pressure; the observed (identical) structure was obtained by two different analysis methods. In addition, the distribution of the peaks does not depend on the radius of the tip.

It was also established that the widths of the peaks and their energy distributions decrease with increasing energy deficit ΔE. The existence of such a structure was observed also for autoionization of neon and carbon monoxide on Mo and Pt tips.

It was initially assumed[23,24] that the observed peaks are due to the existence of so-called virtual surface states, which are connected with the crystal lattice and have a special susceptibility to tunneling. Consequently, the locations of the peaks should vary in a definite manner when the orientation is changed for one and the same sample. Such an assumption was based on the experimental fact that the energy distribution among two neighboring peaks is the same for H_2 and neon. For the first two peaks in the energy distribution of H_2 and Ne, the corresponding difference between the distances from the surface was 3.2 ± 0.5 Å, which is close to the lattice constant of tungsten. However, later more careful experiments performed by Jason[25b] cast definite doubts on such a qualitative explanation. As a result, Jason developed a theory that explained well the observed phenomenon and showed that the resonant peaks in the autoionization have a pure quantum nature. It must be specially emphasized that the theory not only explained the experimentally observed phenomenon, but also a significant next step in the development of a general quantum-mechanical theory of autoionization.

The preceding theories, which did not result in a resonant structure of autoionization, considered the behavior of the tunneling electron only until it reached the metallic surface. Yet its subsequent behavior also turned out to be important, and it was necessary to take into account the potential jump on the vacuum-metal interface. The use of the WKB method, on the other hand, is not justified in this case (since, among other things, the interference effects drop out).

The problem was solved by Jason in the following manner[25b]. The electron in the initial atomic state was described by a wave packet[33], and the exact potential corresponding to the case of autoionization at the metallic surface (dashed lines in Fig. 7) was initially replaced by a simplified potential of rectangular configuration (solid lines in Fig. 7). The rectangular potential barrier (b in Fig. 7) and the potential "step" provide reflecting surfaces analogous to the atomic

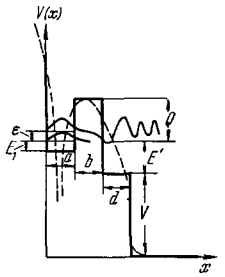

FIG. 7. Simplified diagram of the potential energy (continuous contour) for the case that yields an exact solution that results in a resonant structure [25b].

barrier and the image potential; the space to the right corresponds to the volume of the metal. Further, using the Landau-Lifshitz solution[22] for individual regions (see Fig. 7), one obtains the wave functions $\varphi(\epsilon, x)$, which in this case can be expressed analytically in terms of the following wave numbers:

$$k_1^2 = 2m\hbar^{-2}(E_1+\varepsilon) \quad \text{for region a,}$$
$$k^2 = 2m\hbar^{-2}(Q-\varepsilon) \quad \text{for region b,}$$
$$k_2^2 = 2m\hbar^{-2}(E'+\varepsilon) \quad \text{for region d,}$$
$$k_3^2 = 2m\hbar^{-2}(V+E'+\varepsilon) \quad \text{for the region inside the metal to the right of d.}$$

The values of the wave functions on the boundaries are then equated and "joined" together. The expression obtained in[25b] for the lifetime of the atomic state is

$$\tau = [m(k_1^2+k^2)(1+ka)k_3/8\hbar k_1^2k^3]\,[(1-k_2^2k_3^{-2})(1-k^2k_2^{-2})\cos^2 k_2 d + k_2^2k_3^{-2} + k^2k_3^{-2} + kk_2^{-1}(1-k_2^2k_3^{-2})\sin 2k_2 d]\, e^{2kb}.$$

The result is illustrated in Fig. 8 (a = b = 5 Å, $E_1 + Q$ = 5 eV, U = 8 eV, Q = 3.94 eV, the solid curve corresponds to d = 5 Å and the dashed one to d = 0). As seen from (9), the ionization time is proportional to the time factor e^{2kb} of the WKB expression for the passage of a particle through a potential barrier.

Proceeding to autoionization at the surface of a metal, we now turn to the potential corresponding most closely to the real situation (dashed lines in Fig. 7). Just as in the former simplified case, the main difficulty is to find wave functions of the stable state (we are considering again a hydrogen atom, and the interaction of the charged particles with the flat metallic surface outside the metal is given by the image forces). For the metal we assume the free electron model, i.e., the potential inside the metal is constant at $\varphi - \epsilon_F$ (ϵ_F is the Fermi energy). The equation obtained for the wave functions, in spherical coordinates, is[25b]

$$[-(1/2)\nabla_r^2 - r^{-1} - Fr\cos\theta - (4R)^{-1} - (1/4)(r^2+R^2-2Rr\cos\theta)^{-1/2} + (r^2+4R^2-4Rr\cos\theta)^{-1/2}]\,\varphi(r,\theta,\varepsilon) = (-V_i+\varepsilon)\,\varphi(r,\theta,\varepsilon) \qquad (10)$$

outside the metal and

$$[-(1/2)\nabla_r^2 - FR - (4R)^{-1} - \varphi - \varepsilon_F]\,\varphi(r,\theta,\varepsilon) = (-V_i+\varepsilon)\,\varphi(r,\theta,\varepsilon)$$

inside the metal; here **R** is the vector distance from the mass center of the electron-proton system to the surface, **r** is the vector distance between the electron and the proton, and θ is the angle with the normal to the metal surface. The wave functions were chosen in accordance with the methods proposed in[22].

Since it is impossible to separate the variables in (10), this equation was integrated numerically with a computer. The results are shown in Fig. 9[28]. The

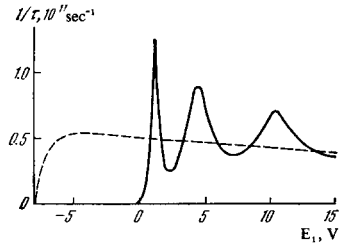

FIG. 8. Ionization probability corresponding to the simplified potential-barrier model, for particles with mass equal to the electron mass, vs E_1 (see Fig. 7, solid curves) [25b].

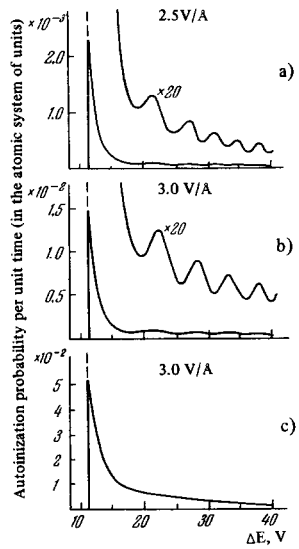

FIG. 9. Dependence of the probability of autoionization of the hydrogen atom with the ionization potential of the H_2 molecule on the energy deficit ΔE.

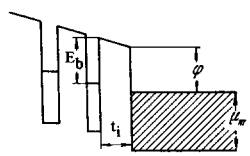

FIG. 10. Simplified diagram of potential energy of an electron near a metallic surface on which an adsorbed particle is present [34].

distributions (a) and (b) are the results of calculation by a theory in which the electron is represented by a wave packet; the distribution (c) corresponds to calculation by the WKB expression. The critical value of ΔE was chosen to be 11.0 eV. It is now appropriate to mention here one more theoretical paper[34] by Alferieff and Duke, who considered the autoionization of an atom near an uneven metallic surface. Replacing the potential curves by rectangular ones (in analogy with the procedure used by Jason[25d]), the presence of an adsorbed atom on the surface of the metal was approximated by them by an additional square well (see Fig. 10, where E_b is the binding energy of the adsorbed particle with the matrix and t_i is the region where the adsorbed atom is located). Examining different cases, the authors of[34] found that the adsorbed atoms can either contribute to the autoionization or decrease its probability. Numerical solutions of the main equation derived by them for the probability of tunneling of an electron from the atom to the metal also yielded resonances. The result corresponding to the case shown in Fig. 10 is illustrated in Fig. 11 (t_i = 1.0 Å; the continuous curve corresponds to E_b = 5 eV and the dashed one to E_b = 0).

We note one other cycle of recent theoretical papers, some conclusions of which can be verified by probe-analysis control experiments. We have in mind the theory of Lucas[35] (a second more complete paper by

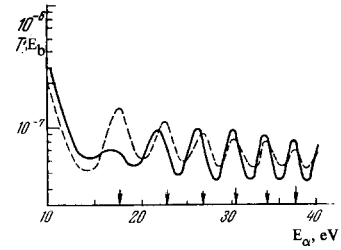

FIG. 11. Electron tunneling probability corresponding to Fig. 10 vs the electron energy [34].

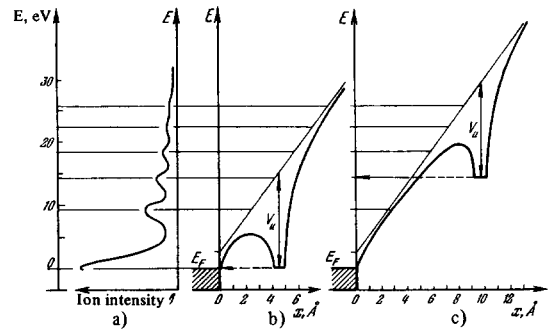

FIG. 12. Distribution of the probability of H_2^+ production (a) in autoionization of hydrogen and plots of the electron potential energy for cases of autoionization at two different distances from the metallic surface, the distance x_c (b) and the distance (c) corresponding to the third peak in the distribution a) [23].

A. Lucas will be published in the Physical Review), according to which the ions produced at the metallic surface lose part of their energy to excitation of surface plasmons during the time of their acceleration at a short distance from the tip[36]. In the case of autoionization, this theory predicts the formation of from one to several plasmons (quanta that excite collective oscillations of valence electrons moving jointly because of their interaction[36a]). This theory is in good agreement with Jason's experimental data[25b] and thus gives a new no-less-convincing explanation of the resonant structure of autoionization. However, the use of the fundamental premises of plasmon theory to describe evaporation by a field leads to results that deviate noticeably from Müller's experiments[3f].

Taking all the foregoing into consideration, the existing picture of image formation[2] in a field-ion microscope can be supplemented (with the stipulation that the described possibilities have different degrees of probability and depend, in addition, on the experimental conditions and on the parameters of the investigated samples) and briefly represented in the following form:

A neutral atom of the image-producing gas approaches the tip at a velocity determined by its thermal motion and dipole attraction. As the atom approaches the surface, the probability of autoionization increases because of the increasing field and the action of the image forces. However, as noted in[23-25], the character of the growth has (as confirmed experimentally for hydrogen and neon) the form shown in Fig. 12a. Figure 12b is a plot of the potential energy of the electron at a distance x_c from the surface, while Fig. 12 shows the case of autoionization at a distance corresponding to the third peak in the distribution of Fig. 12a. Therefore, to the usually discussed cases: (1) autoionization in the "first" ionization band at a critical distance x_c from the

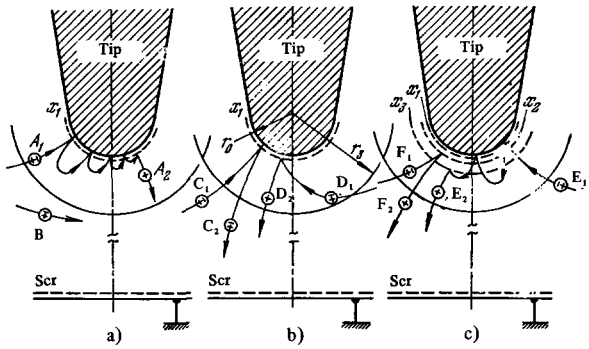

FIG. 13. Scheme of image formation in a field-ion microscope.

surface of the tip (x_1 in Figs. 13a—13c, case A in Fig. 13a) after multiple hops over the surface with gradually decreasing height, (2) autoionization in the "first" ionization band (case C of Fig. 13b) with a second passage through this band after a single collision with the surface of the tip, and (3) autoionization in the "first" ionization band (cases D in Fig. 13b) during its first passage, it is apparently necessary to add also: (4) autoionization in the "second," "third" (cases E in Fig. 13c) etc. ionization bands after multiple collisions of the polarized atom with the surface of the sample, and also cases (5) and (6), which are analogous to the already mentioned possibilities (2) and (3) (cases F in Fig. 13c), but not in the "first" ionization band. The cases F shown in Fig. 13c are apparently incomparably more probable than the cases E (here, as indicated in Chap. 2, much is determined by the value of the applied electric field). It should also be noted that the resolution of the ion images formed in the "second," "third," etc. ionization bands becomes successively worse, and quite sharply at that.

It is possible that the concepts now being developed in connection with the work of Jason et al. will make it possible to interpret finally a large number of effects encountered in practice of field-ion microscopy.

5. PROBE PROCEDURE IN FIELD-ION MICROSCOPY

The most important task of field-ion microscopy is to obtain an unambiguous answer to the question whether a particular bright spot or group of spots observed on the micrograph is the image of a single atom of the sample, a complex of such atoms, an impurity atom (or atoms), atoms or molecules adsorbed on the surface, complicated complexes consisting of foreign substances and atoms, etc. An answer to this question would cast light on many field-ion microscopy problems, still un-

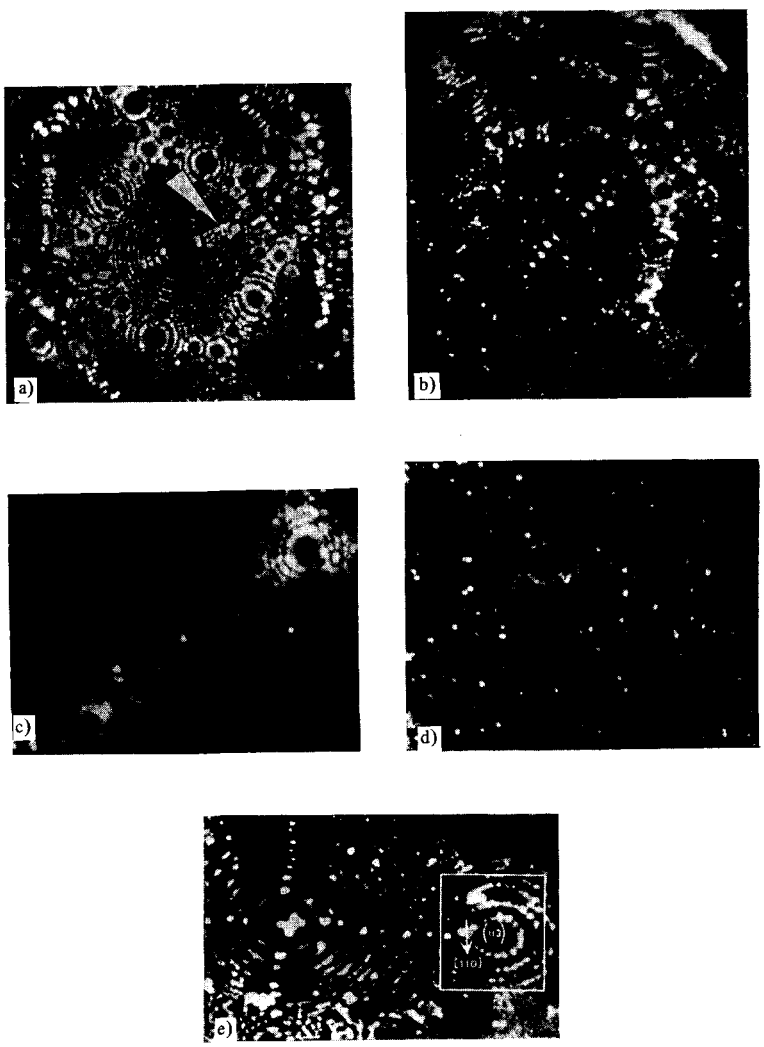

FIG. 14. Points of increased brightness on ion images of metal samples: a) decoration of band lines [001] on the ion image of tungsten [37]; b) alloy W + 1% Gd_2O_3 [37]; c) tungsten sample bombarded by α particles [38]; d) residual-gas molecules adsorbed on the surface of a tungsten tip [39a]; e) dislocation loop [40].

solved in one degree or another. Foremost among them is apparently the question of the nature of the particles that decorate the band lines (for example, the [001] band line on the ion image of field-purified tungsten surface (Fig. 14a)), for in addition to the hypothesis[3b] that field-stabilized low-coordination metastable positions of atoms exist on the surface, there is also the hypothesis that these spots are images of adsorbed gas molecules or complexes of their compounds with the atoms of the tip. This possibility would be even more important in the interpretation of ion images of alloys[37,41a] (Fig. 14b). In addition, knowledge of the nature of the brighter spots on ion images of irradiated samples[9b,38,39a,41b] would permit unambiguous calculation of the concentrations and yield the crystallographic distribution of single displaced atoms and their complexes.

The experimenters have come much closer to the solution of all these (and a few other) problems by developing and steadily improving a new field-ion microscopy procedure, the probe procedure. The prototype of the presently developed perfected instrument[2,8a,42] was the first so-called field-ion microscope atom probe, developed by Müller, Panitz, and McLane[3g,43a,44]. Its schematic diagram is shown in Fig. 15, and constitutes a combination of a field-ion microscope with a time-of-flight mass spectrometer capable of registering individual particles. Its tip is located in the center of revolution of a spherical ground-glass junction, so that a chosen spot on the ion image can be aligned with the probe aperture in the fluorescent screen 6. A high voltage pulse applied to the tip after this procedure detaches the chosen particle from the surface of the sample. This particle, in the form of an atomic or molecular ion, enters the time-of-flight mass spectrometer and is analyzed. The time-of-flight tube with ion detector 4 is located directly under the fluorescent screen and is continuously evacuated by an additional pump 3. The vacuum volume of the instrument is arbitrarily divided into three parts: the part with the tip, to which the image gas is fed, the evacuated region (5) under the fluorescent screen, and the volume of the time-of-flight tube. The evacuation of the system and the admission of the image gas (2) are continuous. (The remaining symbols in Fig. 15 are: 1—manometer, 7—positive high voltage, 8—pulse generator, 9—triggering pulse, 10—oscilloscope, 11—preamplifier.) Metallic versions of this instrument developed by now[8a,42] do not differ in principle at all from the one described

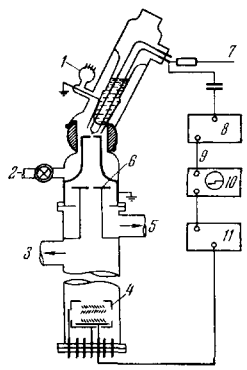

FIG. 15. Diagram of field-ion microscope with atom probe [44].

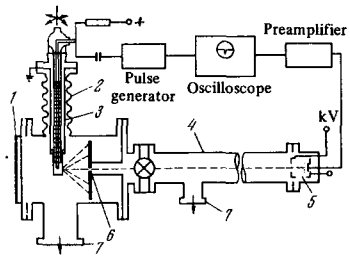

FIG. 16. Diagram of metallic instrument for probe analysis [42].

above (see, for example, Fig. 16, where 1—quartz window, 2—steel bellows, 3—cooled post with emitter tip, 4—time-of-flight tube, 5—ion detector, 6—probe opening in the fluorescence screen, 7—vacuum line).

The atom or complex chosen on the ion image can be evaporated in two ways, either by applying an additional evaporating pulse $V_p^{(+)}$ to the tip, which is at a positive potential V_0 (corresponding to the best image conditions), or else, without changing the tip potential (which is lower than in the first case), by increasing the field intensity at its surface with a negative pulse $V_p^{(-)}$ applied to a nearby ring electrode. The atom (or complex) detached by the pulse V_p traverses in the form of an ion a distance l (on the order of 1 meter) and produces a signal when registered with an electron multiplier. This signal is observed on an oscilloscope, which is triggered by the evaporating pulse. The distance on the oscillogram from the start of oscilloscope operation to the pulse on the multiplier is proportional to the time of flight of the field-evaporated ion. The results of the first investigations were obtained by simplifying the calculations of the ratio of the mass m of the evaporated ion to its charge n. The kinetic energy of the ion, for the case when the duration of the evaporating pulse exceeded the time of stay of the ion in the accelerating field near the tip, was determined from the relation

$$mv^2/2 = ne\,(V_0 + V_p\ ).$$

It is assumed that the field decreases rapidly with increasing distance from the tip and that the ion acquires its entire energy in a path section in the immediate vicinity of the tip, after which it moves with constant velocity in a field-free region. The time of flight is then approximately equal to

$$\tau \approx l/v$$

and

$$(m/n)_0 = 2e\,(V_0 + V_p\ )\,\tau^2/l^2. \qquad (11)$$

This formula, however, does not take into account a number of factors. Thus, if an ion with energy $ne(V_0 + V_p)$ is accelerated while still at the input to the multiplier by a field corresponding to the potential V(x), then formula (11) is replaced by

$$m/n = [2e\,(V_0 + V_p\ )\,\tau^2/l^2]\,\beta = (m/n)_0\beta,$$

where

$$\beta \equiv \left\{ d^{-1} \int_0^l [1 + V(x)\,(V_0 + V_p\ )]^{-1/3}\,dx \right\}^2; \qquad (12)$$

here x is the distance from the detector. The calculation of the integral in (4) calls for preliminary experimental determination of the actual distribution of the field at the detector.

Another error-producing factor is the strong influence exerted by the stray fields on the ion energy. In addition, the ion trajectory can be strongly altered by the flight components of the field near the tip, and this results in registration of another (non-analyzed) ion. The tip of such an instrument must therefore be well screened. In addition, one should add to formula (11) two correction factors[42], namely the coefficient pulsed-voltage coefficient ω, which accounts for the fact that if the evaporating pulse is long enough the reflected voltage wave enhances the pulse amplitude (by a factor ω), and the total delay time δ of the measuring circuit, accounting for the fact that the inherent delays cause the electronic circuit to measure not the true time of flight but

$$t = \tau \pm \delta.$$

As a result we have

$$(m/n)_0 = 2e\,(V_0 + \omega V_p)\,(t \pm \delta)^2/l^2. \qquad (13)$$

The method of determining the correction factors ω and δ is an independent problem. Müller et al.[42] proposed to calibrate the probe instruments against materials that produce in the case of field evaporation a known type of ion. Most frequently, a field-ion microscope with atom probe is calibrated by using tips of rhodium, a metal having a single isotope.

If evaporating pulses are continuously applied to such a tip, then two mass peaks corresponding to the same instants of time are observed on the oscillogram (see, e.g., Fig. 17); they can represent only rhodium ions with different charges (the peak shown below the time scale corresponds to mass 4 (adsorbed helium)). Writing down Eq. (13) for each of the registered masses and dividing term by term, we obtain

$$(m/n)_2/(m/n)_1 = t_2^2[1 \pm (\delta/t_2)]^2/t_1^2[1 \pm (\delta/t_1)]^2 \approx t_2^2[1 \pm (2\delta/t_2)]/t_1^2[1 \pm (2\delta/t_1)]. \qquad (14)$$

Putting in (14) $\delta = 0$ as a first approximation, the authors of[42] found that for a rhodium sample the ratio m/n for doubly- and triply-charged ions is $(m/n)_2/(m/n)_1 = 1.5$. The correction factors ω and δ were determined from the expressions

$$\omega = \{[(m/n)_2]^{1/2} - [(m/n)_1]^{1/2}\}^2\, l^2(2eV_p\Delta t^2)^{-1} - (V_0/V_p) \qquad (15)$$

and

$$\delta = t_2 - \Delta t\,\{1 - [(m/n)_1/(m/n_2)]^{1/2}\}^{-1},$$

where $\Delta t = t_2 - t_1$ is the time interval between the peaks of the two masses. The value of ω determined in[42] was 2.00 ± 0.05. It does not depend on the masses chosen for the calibration, but is determined to a considerable degree by the geometry of the transmission-line ring. If it is assumed that the errors in the measurement of the quantities V_0 and V_p are negligibly small, then the relative error in m/n, determined from (13), is

$$\Delta(m/n)_0/(m/n)_0 = V_p/(V_0 + \omega V_p)\,\Delta\omega + 2(t + \delta)^{-1}(\Delta t + \Delta\delta).$$

According to the data of[42], the error $\Delta\omega$ is usually equal to ± 0.05, and $\Delta\delta = 0.02$. On the other hand, the error Δt amounts to 0.02, owing to the instability of the oscilloscope sweep, so that for ions with $V_0 + \alpha V_p = 10$ kV and $V_p = 1$ kV the mass measurement error is approximately equal to ± 0.6 a.m.u. at $(m/n)_0 = 20$ a.m.u. and ± 1.6 a.m.u. at $(m/n)_0 = 100$ a.m.u.

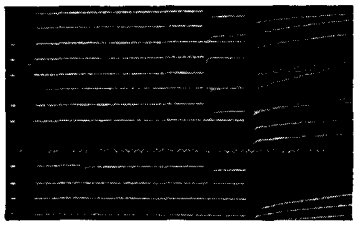

FIG. 17. Peaks of the ions Rh^{3+} and Rh^{2+} at 21°K and 5×10^{-8} mm Hg ($V_0 = 14.8$ kV, $V_p = 2.0$ kV) [42].

If the same oscillogram shows several peaks with different masses, one of which can be exactly identified, then the other masses can be calculated from the Eq. (15), and the resolution is then greatly improved.

The first results obtained so far with a field-ion microscope with atom probe did not take into account the corrections indicated above, i.e., they were obtained without calibration. Without detracting from their importance, such data are useful more readily for the development of the method than for pure reference purposes.

A field-ion microscope with atom probe was used in[42] to observe, by field evaporation of tungsten tips, the complexes $(W^{182}O_2^{16})^{3+}$ and $(W^{184}O_2^{16})^{4+}$ (the ratios m/n were 71.3 and 54.0, respectively).

The obtained m/n ratios could also be identified (taking into account the poor vacuum conditions near the tip) as $(W^{186}N_2^{14})^{3+}$ or $(W^{186}N_2^{14})^{4+}$ or else $(W^{182}N_2^{14})^{3+}$. For the latter complex we have m/n = 71.2.

An investigation of an Re—Mo alloy has shown that field evaporation produces the ions $(Mo^{96})^{2+}$ and Re^{2+}, corresponding to m/n = 48 and 93.

Investigations of pure tungsten (at 21° K) yielded m/n = 66 and 91. The ratio m/n = 91 is interpreted as corresponding to $(W^{182})^{3+}$, while m/n = 66 corresponds to $(W^{182}O^{16})^{3+}$ or $(W^{184}N^{14})^{3+}$. In certain cases, the obtained m/n ratios were 60.9 and 64.6. They could be ascribed to $(W^{186})^{3+}$ – (m/n = 62), $(W^{182}N^{14})$ – (m/n = 65.3) or $(W^{182}O^{16})^{3+}$ – (m/n = 66). W^{2+} ions were observed in rare cases, but the data obtained in[42] did not lead to reliable conclusions concerning the relative effectiveness of W^{2+} and W^{3+} ion formation.

We mention also Brenner and McKinney's earlier investigations of the products of field evaporation of tips of pure W and Ir,[8b,8c,45] using a field-ion microscope with an atomic probe. In[8c] they used a metallic construction, a somewhat simplified variant of the system shown in Fig. 16. The instrument made it possible to observe the ion image of a surface of the investigated sample and to photograph it. It was established that Ir is evaporated predominantly in the form of Ir^{2+}. Ir^{3+} ions were also observed, and the ratio of the number of doubly- and triply-charged ions was independent of the temperature, something difficult to reconcile with the existing concepts. The tungsten was evaporated in the form of triply-charged ions. What is particularly surprising is (as noted by the authors themselves) that no temperature dependence of the ratio of the ion types produced in field evaporation was observed (down to 30° K and below).

The results obtained by Brenner and McKinney[8C] are contradictory in many respects, a fact that can be apparently attributed to two causes. First, errors can be caused by the fact that the ratios m/n were calculated by a very approximate formula of the type (11), and second, the absence of tip screening also plays a role. In addition, a shortcoming of the design used in[8C] is the use of an unscreened ring, to which a negative pulse is applied, for the evaporation of the surface atoms of the tip. Such a scheme, as indicated by the authors of[42], makes it very difficult to direct the evaporated atom into the opening of the analyzer, so that the identity of the type of atom observed on the ion image becomes doubtful. The previously observed increase in the charge of a metal ion when it is evaporated by a field, was confirmed also by other experimenters[3c,d,i,j] and was the first important (and unexpected) result of the use of the probe procedure. W, Ta, and Ir were evaporated in the form of triply- and quadruply-charged ions[3i,8C]. Evaporation in the form of triply-charged ions was observed also for Pt, Rh, Au, and Fe[3d,i] and in the form of quadruply charged ions for Mo, Re, and Nb[3d,i]. In all cases, the relative number of the evaporated ions with higher charge increased with increasing rate of evaporation, which can be raised[7] to 10^9 atomic layers per second.

It is of great interest to establish that the image gas is adsorbed on the surfaces of metallic needle-shaped samples[3i,8d,43b] at field intensities corresponding to the conditions of the best surface image. This result was particularly unexpected for He, Ne, and Ar, for according to the earlier concepts[3a,b] the adsorption of these gases (He most strongly, followed by Ne and Ar, and H to the least degree) should not take place in this case. Müller et al. observed later on that to desorb noble gases adsorbed on the tip surface it is necessary to apply fields sufficient for simultaneous evaporation of the metal atoms situated in the layer in which the adsorbed atom is located. In practice this effect is revealed by the fact that the evaporating fields are weaker in the presence of noble gases than in vacuum.

The cited studies call for a review of both the process of image formation in the field ion microscope and of the theory of ion production at metal surfaces in general. Among these investigations, notice should be taken first of the latest (known to the authors) paper of Müller et al. (see[46]). It describes an experimental verification of a hypothesis advanced somewhat earlier[3k,19c], that an adsorbed atom of the image gas ("cap") covers each of the atoms that protrude most from the surface of the tip, and that the maximum ionization probability occurs when the incoming atom of the image gas touches the adsorbed atom. The gist of this experiment reduced to the following: The dimension of the probe opening was chosen to be somewhat larger than usual, in order that not one but several image atoms fall in its "shadow." Further, the usual scheme was used to register the particles passing through the probing aperture (the oscilloscope sweep, 20 and 100 μsec, was triggered in this case by a pulse from an external source). Under normal conditions of best surface image in helium ions, 5—6 particles (peaks on the oscillogram) from three image atoms on the surface were registered within 20 μsec on the collector (multiplier) of the time-of-flight tube. The measurements were then performed in a pulsed regime with a sweep time 100 μsec. In this case the oscilloscope was triggered by the evaporating pulse itself.

The result was a strong decrease in the number of particles arriving at the collector, which, however, was restored after ~ 10—20 μsec. Calculations performed by the authors of[46] have shown that this is just the time necessary for adsorption of new atoms of the image gas and for additional atoms that become ionized over the newly produced "caps," to reach the surface of the tip. The measurements were made for different (three) pressures of the image gas; the effect was confirmed in all cases. The result does not alter significantly the qualitative picture of the formation of the field-ion image: it does not exclude, for example, the idea of "hops" of polarized particles over the surface of the tip (although the number of such "hops" should decrease considerably when the accommodation coefficient is increased), and does not disaffirm the experimentally observed resonance structure of the ionization. Nonetheless, the fundamental theories will have to be reviewed, and this will concern to a greater degree the theory of desorption and evaporation by a field, for according to the present concepts a field-purified tip surface remains atomically pure during the entire time of application of the field producing the best image of the surface in helium ions. (Tsong and Müller[19b] have recently shown that the adsorption of inert-gas atoms is due to dipole-dipole interactions stimulated by a strong electric field.) It can also be assumed that this result will make it possible to explain more correctly many effects observed in field-ion microscopy practice. The publication of such papers should be expected in the nearest future.

Müller, Krishnaswamy, and McLane[7] investigated the influence of different image gases on the character of the field evaporation of Ta, Rh, Mb, Au, W, and Ir and analyzed the formation of molecular ions of the image gases and metal surface atoms in the case of evaporation by the field. The most thoroughly investigated was the behavior of Ta. A metallic instrument[10] was used for the analysis (see Fig. 16), with a mass resolution 250. In the analysis with the atom probe (at the best surface-image voltage), tantalum shows preferred production of Ta^{3+} ions (60.33 a.m.u.), a somewhat smaller number of Te^4 (45.20 a.m.u.), and some amount of Te^{2+} (90.5 a.m.u.). The presence of hydrogen decreased the evaporating field for Ta. The main product of Ta evaporation in the presence of hydrogen is the triply-charged hybrid molecule TaH^{3+}, which can decay (dissociate) in accordance with the reaction

$$TaH^{3+} \rightarrow Ta^{2+} + H^+. \qquad (16)$$

The picture can be visualized in this case as follows: The molecular ion TaH^{3+} is desorbed by the evaporating pulse from the surface of the tip and is accelerated away from the tip to distance d, where it dissociates in accordance with Eq. (16). The two produced ions (Ta^{2+} and H^+) then move under the influence of a lower voltage V_d (in comparison with the potential at the surface of the tip) at a velocity v_e. Far from the tip, in the region arbitrarily considered to be free of the field, the

ion velocities are $v_e^{(Ta)}$ and $v_e^{(H)}$. The final kinetic energies of these ions are

$$0.5m_H(v_e^H)^2 = 0.5m_H v_d^2 + e(v_e - v_d), \quad (17)$$

$$0.5m_{Ta}(v_e^{Ta})^2 = 0.5m_{Ta}v_d^2 + 2e(v_e - v_d). \quad (18)$$

The velocity v_e at the instant of dissociation is determined from the relation

$$0{,}5m_{TaH^{3+}}v_d^2 = 3ev_d. \quad (19)$$

The apparent mass M of the dissociation products, measured in a time-of-flight tube, is

$$M = 2eV_e/v_e^2, \quad (20)$$

where $V_e = V_0 + V_p$. Substituting (19) and (20) in (17) and (18), we obtain

$$M_{H^+} = m_H m_{TaH} V_e/[3m_H V_d + m_{TaH}(V_e - V_d)],$$
$$M_{Ta^{3+}} = m_{Ta} m_{TaH} V_e/[3m_{Ta}V_d + 2m_{TaH}(V_e - V_d)].$$

As shown by the authors of[7], the decay (dissociation) of the TaH^{3+} ion occurs in the strong-field region near the surface of tip. Approximating the distribution of the potential in the accelerating region by the potential between two confocal paraboloids of revolution

$$V_r = V_e\{1 - \ln(R/r)[\ln(R/r_0)]^{-1}\}, \quad (21)$$

where the coordinates of the ion flight are measured from the focal point, the authors of[7] calculated the distance d from the surface of the tip, on which the dissociation takes place, and also the time t′ after which the TaH^{3+} ion traverses this distance. In (21), R is the distance from the surface of the tip to the accelerating electrode (0.1 cm), and r_0 is the radius of the tip. The distance x from the surface of the tip is equal to $r - 0.5r_0$. The indicated time t′ was obtained by numerical integration

$$t' = \int_0^d v_x^{-1}\,dx,$$

where the ion velocity v_x was calculated from the expression

$$v_x = (6eV_x/m_{TaH})^{1/2}.$$

The results obtained in the described case are shown in Figs. 18a and b. As seen from these figures, the dissociation probability is maximal at distances from the surface on the order of the radius of the tip. At large distances, dissociation does not take place at all, as confirmed by the remaining small amount of the TaH^{3+} (60.7 a.m.u.). It should be noted that the total number of observed particles (238 for Fig. 18a and only 29 for Fig. 18b) may not be sufficient to overcome the statistical fluctuations.

Field evaporation of Ta in the presence of He led in the overwhelming majority of cases to the formation of the ions $TaHe^{3+}$. We note that the products of field evaporation of certain metals in He were investigated earlier by Müller[3k] for rhodium and by Müller et. al.[43b] for tungsten, iridium, and iron tips.

In the case of helium adsorption, the metal is frequently evaporated in the form of molecular ions such as WHe^{3+}, WHe_2^{3+}, $IrHe_2^{3+}$, $IrHe_2^{2+}$, $RhHe^{2+}$ and $FeHe^{2+}$.

Evaporation of Ta in neon produced Ta ions with charges from 1 to 4 and singly-charged Ne ions (20 and

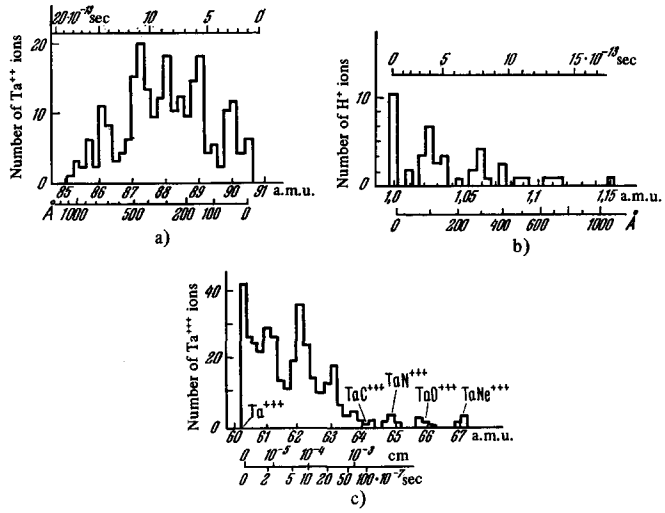

FIG. 18. Distribution of Ta^{2+} (a) and H^+ (b) ions in the dissociation of the molecular ions TaH^{3+} produced by field evaporation of a tantalum tip in the presence of hydrogen, and distribution of the Ta^{3+} ions (c) obtained by field evaporation of a tantalum tip at 78°K in the presence of Ne ($p_{Ne} = 10^{-4}$ mm Hg) [7].

22 a.m.u.). About 10% of the ions were doubly charged and 1% of the ions were in the form of Ne_2^+ (40 a.m.u.). The total number of molecular TaNe ions (with charges from 2 to 4) was ~ 1% of a total number of registered particles. An appreciable number of particles had apparent masses above 60.33 a.m.u., corresponding to the Ta^{3+} ion (see Fig. 18b). These ions can be interpreted as the dissociation products of the unstable molecular ion $TaNe^{3+}$:

$$TaNe^{3+} \rightarrow T^{3+} + Ne.$$

The apparent masses $M_{Ta^{3+}}$ and M_{Ne}, and also the distances over which dissociation takes place and the time preceding the dissociation (from the instant of evaporation of the molecular ion), were determined by the procedure described above for hydrogen. The presence of residual hydrogen delayed the formation of the $TaNe^{3+}$ ions, owing to adsorption of the hydrogen on the surface of the metal. In addition, we observed formation of NeH^+ ions in the presence of residual hydrogen.

Brenner and McKinney[8a], using a metallic probe instrument constructed by them, analyzed certain alloys (Fe + 3.8% Pt + 20% Ni, Fe + 1.55% Cu, and Fe + 4.9% Mo) and found a surprisingly good agreement between the alloy composition deduced in this manner and the real composition. The result obtained for the Fe + 4.9% Mo alloy is shown in Fig. 19.

In addition, the same authors analyzed the mass spectra of alloys containing divalent iron at different temperatures and vacuum conditions. In the case of the image of Fe + Mo alloy in Ne ($p_{Ne} = 2.4 \times 10^{-5}$ mm Hg), the field-evaporation mass spectrum obtained at 30°K

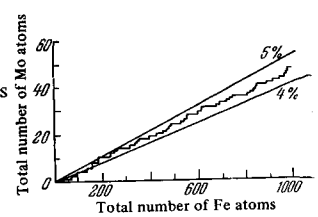

FIG. 19. Results of probe analysis [8a] of a certain arbitrarily chosen region of the dilute alloy Fe + 4.9% Mo.

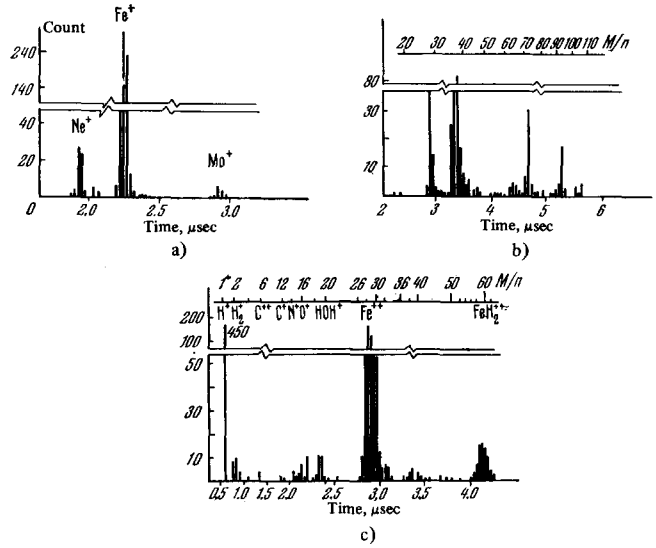

FIG. 20. Spectra obtained in a probe analysis [8a] of an Fe + Mo alloy in the presence of neon (T = 30°K, p_{Ne} = 2.4 × 10^{-5} mm Hg) (a), under conditions of high vacuum at T = 300°K (b), and after soaking in H_2 at T = 80°K (c).

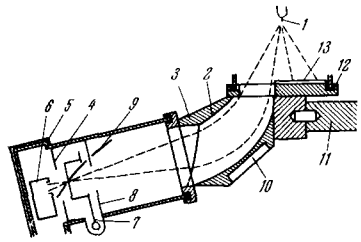

FIG. 21. Diagram of instrument for mass spectrometric analysis of field-evaporation products [47a].

contains mainly peaks corresponding to the ions Fe^{2+}, Mo^{2+}, and Ne^+ (Fig. 20a). Almost all 700 registered particles represented one of the indicated types of ions. Field evaporation of the same samples at room temperature in a vacuum better than 10^{-8} mm Hg gives a complicated spectrum, in which FeO or FeOH ions predominate. Contamination of the surface, even at liquid-nitrogen temperature, leads to the appearance of complicated spectra. This can be seen from an examination of the spectrum of the indicated alloy (Fig. 20c), obtained after obtaining its image in hydrogen at T = 80°K.

A field ion microscope with atom probe, somewhat different from that described above and intended for mass spectrometric analysis of autoionization and field evaporation products, was designed by Barofsky and Müller[2,47]. A schematic diagram of this instrument is shown in Fig. 21 (1—tip sample, 2—iron sector lens (solid lines), 3—brass filling, 4—collimator, 5—iron magnetic screen, 6—electron multiplier, 7—focusing slit, 8—collimator, 9—focusing plate, 10—slot for support, 11—heated rod, 12—ring, 13—fluorescent screen). The high resolution (90 a.m.u.) is obtained here by maintaining the ion energy constant. The ions emitted from the tip pass through the slit of the mass spectrometer and are focused in the usual manner by the magnetic field. The energy of the ions corresponds to a constant voltage on the tip and does not depend on the

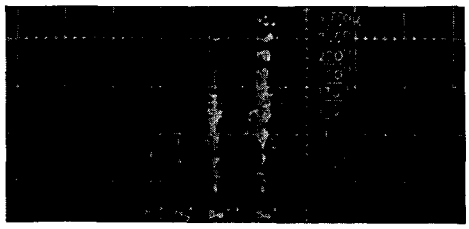

FIG. 22. Mass spectrogram of field evaporation of beryllium at different temperatures [47a].

potential of the accelerating electrode. At a given magnetic field, the detector is reached by ions having a definite ratio e/M. Among the many conveniences (advantages) of such an instrument, the authors of[47] list the absence of activated surfaces (as is the case with an instrument with a time-of-flight tube). This is very important from the point of view of the possible harmful effect of the atmosphere (air) when it is necessary to open the instrument periodically. The signal received by the detector is amplified and fed to an oscilloscope. The vertical deflection of the oscilloscope beam is produced by a converted accelerating voltage; the horizontal deflection is connected in a definite manner with the variation of the magnetic field. The series of the mass spectra obtained on the oscilloscope screen are photographed. A typical mass spectrum corresponding to field evaporation at different temperatures is shown in Fig. 22. The mass scale is usually calibrated with the aid of autoionization of noble gases (H_2, Ne, Ar, Kr). The instrument can register ions of the image gas at a pressure p = 10^{-7} mm Hg and at a count of 10 a.m.u./sec, corresponding to an evaporation rate on the order of 3 atomic layers per second. Under such conditions, 100 ions of the evaporated metal reach the detector each second.

The described instrument was used by Barofsky and Müller (see[47,48]) for a mass spectrometric analysis of the products of low-temperature field evaporation of Fe, Co, Ni, Be, Cu, and Zn. All these metals yielded at low temperatures singly- or doubly-charged ions (Fe^{2+}, Be^{2+}, Cu^+, Cu^{2+}, Zn^+, Zn^{2+}, Co^{2+}, Ni^{2+}); formation of different molecular ions was observed at higher temperatures.

6. CONCLUSION

It may be stated at present that the mass-spectrometry procedure plays a tremendous role in the development of both theoretical and practical aspects of field-ion microscopy. Tremendous importance is attached at the present time to the use of the probe procedure, which by now has passed the research and development stage and can provide new information of independent importance. Many of the results, already known as well as envisioned in the nearest future, could not be (and cannot be) obtained by means not connected with mass spectrometry. Even the observation of molecular ions of certain types in strong electric fields, is a fact of independent interest, since the existence of such ions was not predicted or observed earlier. One of the most important results is the observation of the adsorption "layer" of the image gas, contributing to autoionization. We note also that the probe analysis of surfaces of tips

becomes very important because of the possible influence of adsorption of the image gas on the character of the preferred field evaporation of samples in the field ion microscope, an influence that cannot be neglected[7].

The probe procedures indicated in the beginning of Chap. 5 are barely in the initial development stage, and prolonged and painstaking work is anticipated in this field.

The authors are deeply grateful to G. M. Kukavadze for help with writing the article, for useful advice, and remarks.

[1] F. A. White, Mass Spectrometry in Science and Technology, N. Y., J. Wiley, 1968, ch. 3.

[2] E. W. Müller and T. T. Tsong, Field-ion Microscopy, Principles and Applications, N. Y. Elsevier, 1969, chs. II. 5, III. 6, IV. 6 and VII. 7.

[3] E. W. Müller, a) Adv. Electron. and Electron Phys. 13, 831 (1960); b) Science 149, 591 (1965); c) Adv. Mass. Spectrometry 5, 427 (1971); d) Naturwiss. 57, 222 (1960); e) Phys. Rev. 102, 618 (1956); f) Ber. Bunsen. Ges. phys. Chem. 75, 979 (1971); g) 15th Field Emission Symposium. Proc. (Bonn, 1968), Bonn, 1969, p. 108; h) Quart. Rev. 23, 177 (1969); i) Applications of FIM in Physical Metallurgy and Corrosion, ed. by F. R. Hochman et al., Georgia Inst. of Technology, 1969, p. 59; j) J. Vac. Sci. Techn. 8, 89 (1971).

[4] a) H. D. Beckey et al., Adv. Mass Spectrometry 3, 35 (1966); H. D. Beckey, ibid. 2, 1 (1963); b) Field Ionization Mass Spectrometry, Oxford, Pergamon Press, 1970, chap. I.

[5] A. J. B. Robertson and B. W. Viney, Adv. Mass. Spectrometry 3, 23 (1966).

[6] I. V. Gol'denfel'd, 1-ya Vsesoyuznaya konferentsiya po mass-spektroskopii (First All-union Conference on Mass Spectroscopy) (Leningrad, 1969), ANSSSR, 1969, p. 337; Abstract of doctoral dissertation, M., 1971.

[7] E. W. Müller, S. V. Krishnaswamy and S. B. McLane, Surface Sci. 23, 112 (1970).

[8] S. S. Brenner and J. T. McKinney, a) ibid., p. 88; b) cm.[3], p. 111; 16th Field Emission Symposium, Proc., Pittsburgh, Pa., 1969; c) Appl. Phys. Lett. 13, 29 (1968); d) Surface Sci. 20, 411 (1970).

[9] a) M. J. Southon, in: Field-ion Microscopy, Plenum, 1968, Chap. 2; A. L. Suvorov, ibid., Russ. transl., Mir, 1971, p. 246; b) Usp. Fiz. Nauk 101, 21 (1970) [Sov. Phys.-Uspekhi 317 (1970)].

[10] G. Gamow, Zs. Phys. 51, 204 (1928).

[11] J. R. Oppenheimer, Phys. Rev. 31, 67 (1928).

[12] C. Lanczos, Zs. Phys. a) 62, 518; 65, 431 (1930); b) 68, 204 (1931).

[13] H. A. Bethe and E. Salpeter, Handb. Phys., Bd. 35, Springer-Verlag, 1957, S. 88.

[14] R. H. Good and E. W. Müller, ibid., Bd. 21, 1956, S. 176.

[15] D. Bohm, Quantum Theory, Prentice-Hall, 1951, Chap. 12.

[16] D. S. Boudreaux and P. H. Cutler, a) Solid State Comm. 3, 219 (1965); b) Surface Sci. 5, 230 (1966); c) Phys. Rev. 149, 170 (1966).

[17] S. P. Sharma, et al., Surface Sci. 23, 30 (1970).

[18] N. F. Mott and H. S. W. Massey, Theory of Atomic Collisions, Oxford, 1965.

[19] T. T. Tsong and E. W. Müller, a) J. Chem. Phys. 41, 3279 (1964); b) J. Chem. Phys. 55, 2884 (1971); c) Phys. Rev. Lett. 25, 911 (1970).

[20] I. V. Gol'den'feld et al., Intern. J. Mass. Spectr. Ion Phys. 5, 337 (1970).

[21] M. H. Rice and R. H. Good, J. Opt. Soc. Am. 52, 239 (1962).

[22] L. D. Landau and E. M. Lifshitz, Kvantovaya mekhanika (Quantum Mechanics), 2nd ed., M., Fizmatgiz, 1963, Sec. 24 [Addison-Wesley, 1965].

[23] A. J. Jason et al., J. Chem. Phys. 44, 4351 (1966).

[24] A. J. Jason et al., ibid. 43, 3762 (1965).

[25] A. J. Jason, a) Proc. of the 13th Field Emission Symposium, Cornell University, 1966, p. 62; b) Phys. Rev. 156, 266 (1967).

[26] R. Gomer and L. W. Swanson, J. Chem. Phys. 38, 1613 (1963).

[27] D. G. Brandon, a) Brit. J. Appl. Phys. 14, 474 (1964); Surface Sci. 3, 1 (1965); Phil. Mag. 14, 803 (1966); b) see[9a], p. 34.

[28] T. T. Tsong, Surface Sci. 10, 102 (1968).

[29] L. N. Dobretsov and M. V. Gomoyunova, Emissionaya elektronika (Emission Electronics), Nauka, 1966, Chap. 10.

[30] N. I. Ionov, Zh. Tekh. Fiz. 39, a) 716, b) 721 (1969) [Sov. Phys.-Tech. Phys. 14, a) 538, b) 542 (1969)].

[31] M. G. Inghram and R. Gomer, a) J. Chem. Phys. 22, 1279 (1954); b) Z. Naturforsch. 10a, 863 (1956).

[32] E. W. Müller and K. Bahadur, Phys. Rev. 102, 624 (1956).

[33] E. Fermi, Nuclear Physics, Univ. of Chicago, 1950, Chap. IV; I. I. Goldman, Problems in Quantum Mechanics, ed. by D. ter Haar, L., Inforsearch, 1960, p. 202.

[34] M. E. Alferieff and C. B. Duke, J. Chem. Phys. 46, 938 (1967).

[35] A. A. Lucas, Phys. Rev. Lett. 26, 813 (1971).

[36] D. Pines, a) Rev. Mod. Phys. 28, 184 (1956); in: Elementary Excitations in Solids, N. Y., Benjamin, 1964, p. 100.

[37] A. L. Suvorov and V. A. Kuznetsov, Fiz. Met. Metallov. 27, 566 (1966).

[38] A. L. Suvorov, G. M. Kukavadze, and A. F. Bobkov, Zh. Eksp. Teor. Fiz. 58, 85 (1970) [Sov. Phys.-JETP 31, 47 (1970)].

[39] A. L. Suvorov and G. M. Kukavadze, a) in: Monokristally tugoplavkikh i redkikh metallov (Single Crystals of High Melting Point and Rare Metals), M., Nauka, 1971, p. 108; Fiz. Met. Metallov. 28, 238 (1969); b) 30, 116 (1970).

[40] M. A. Fortes, et al., Phil. Mag. 17, 169 (1968).

[41] a) V. A. Kuznetsov, G. M. Kukavadze and A. L. Suvorov, in: Reniĭ v novoi tekhnike (Rhenium in New Technology), Nauka, 1970, p. 108; B. Ralph, Surface Sci. 23, 130 (1970); cf.[9a], p. 161, b) p. 176.

[42] J. A. Panitz et al., Rev. Sci. Instr. 40, 1321 (1969).

[43] a) E. W. Müller and J. A. Panitz, 14th Field Emission Symposium, Proc., Washington, D. C., 1967; E. W. Müller, S. B. McLane and J. A. Panitz, 15th Field Emission Symposium. Proc. (Bonn, 1968), Bonn, 1968, p. 110; b) Surface Sci. 17, 430 (1969).

[44] E. W. Müller, J. A. Panitz and S. B. McLane, Rev. Sci. Instr. 39, 83 (1968).

[45] S. S. Brenner, High Temperature Resolution

Metallography, ed. by H. I. Aaronson and G. S. Annsell, N. Y., Gordon and Breach, 1967, p. 281.
[46]S. B. McLane et al., ibid. 27, 367 (1971).
[47]D. F. Barofsky and E. W. Müller, a) ibid. 10, 177 (1968); b) Intern. J. Mass. Spectr. Ion Phys. 2, 125 (1969).
[48]D. F. Barofsky, ibid. 3, 156 (1969).

Translated by J. G. Adashko